Role of the electrostatic depletion attraction on the structure of charged liposome-polymer mixtures

M. Peláez-Fernández,[1] A. Moncho-Jordá,[1] S. García-Jimeno,[2] J. Estelrich,[2] and J. Callejas-Fernández[1]
[1]*Grupo de Física de Fluidos y Biocoloides, Departamento de Física Aplicada, Facultad de Ciencias, Universidad de Granada, E-18071 Granada, Spain*
[2]*Departament de Fisicoquímica, Facultat de Farmàcia, Universitat de Barcelona, E-08028 Barcelona, Catalonia, Spain*
(Received 26 July 2011; revised manuscript received 14 December 2011; published 29 May 2012)

The effect of adding charged nonadsorbing polymers to electrostatically structured suspensions of charged liposomes has been experimentally studied by means of light scattering techniques. The static structure factor of the mixtures is analyzed using two polymers of different sizes. As the polymer concentration increases, the main peak of the structure factor decreases and shows an important shift to larger values of the scattering vector. Such displacement is the consequence of the electrostatic-enhanced depletion attraction induced by the polymers that counteracts the electrostatic repulsion. For the shorter polymer, the system remains stable for all studied polymer concentrations. However, for the long polymer chains, the effective attraction induced at the highest polymer density studied is strong enough to destabilize the mixture. In this case, the aggregation of the liposomes leads to clusters of nearly linear morphology. The PRISM theory is employed to calculate the effective pair potential between liposomes. The theoretical predictions are able to support the experimental observations, and provide an explanation of the interplay between the electrostatic repulsive interaction and the depletion attraction. In particular, they show that the depletion attraction is especially long ranged, and is dominated by electrostatic effects rather than entropic.

DOI: 10.1103/PhysRevE.85.051405 PACS number(s): 82.70.Dd, 61.20.−p

I. INTRODUCTION

Complex fluids are usually found in technological products, biological fluids, foods, etc. They are formed by mixtures of different types of colloids (synthetic particles, proteins, polymers, ...). The characterization and knowledge of binary mixtures, i.e., two components immersed in a solvent, represents a first step in a further comprehension of those more complex systems. One of the most studied binary mixture is formed by neutral sterically stabilized colloids and nonadsorbing polymers [1–3]. Simulation and experimental results show that the presence of neutral polymers in a colloidal sample has a deep impact on the structural and dynamical properties that leads to a very rich phenomenology, such as fluid-fluid phase separation and formation of gels or attractive glasses [4–9]. For these mixtures, the driven mechanism is the excluded volume repulsion between colloids and polymers that induces the well-known entropic depletion attraction between colloids [10,11]. For mixtures of charged colloidal particles and uncharged polymer coils, there is a competition between the long-range electrostatic repulsion and the short-range entropic depletion attraction. For these systems, the colloidal structure goes from electrostatically stabilized colloidal clusters to the formation of attractive gels [5,12–19].

In the last years, attention has been driven to colloid-polymer mixtures where both species are like-charged. Mixtures of charged particles are involved in many real systems, where the stability of the suspension is also determined by the depletion forces [20–22]. However, the main difference from uncharged binary systems relies on the fact that attractive depletion interactions are now affected by the electrostatic repulsion between particles. For the particular case of charged colloid-polymer mixtures, the effective depletion attraction between colloids becomes greatly enhanced by the colloid-polymer electrostatic repulsion. The existence of this effect has been confirmed theoretically [23], by means of computer simulations [24], and in experiments [25–30]. The resulting depletion attraction arising in this kind of systems is very strong even at small polymer concentrations, where the entropic depletion is negligible. Moreover, its range can be tuned by changing the electrolyte concentration in the suspension and the polymer radius of gyration, R_g. In the limit of very low ionic strength, the range of the electrostatic depletion can further exceed the polymer diameter $2R_g$ and control the structural behavior of the sample.

Recently, we have studied diluted but structured colloidal dispersions of charged and monodisperse latex model particles at low ionic strength, and showed that the attractive depletion interaction induced by the charged polymers is dominated by the electrostatic part [28,29]. In the current article, we extend this experimental study to dense colloidal suspensions (up to the packing fraction of $\phi_c = 0.17$) at larger polymer concentrations. For these concentrations, the entropic (excluded-volume) effects arising in charged colloid-polymer mixtures could also appear and overlap with the electrostatic ones, so the depletion attraction can depend on both contributions [7,8,13].

In this work we employ charged liposomes as colloidal particles and like-charged nonadsorbing polymers immersed in water. From an experimental point of view, liposomes are spherical particles formed by a very thin layer, and so they have a refractive index very close to the solvent. This property allows the use of light scattering techniques even at very large particle volume fractions, which cannot be reached with hard colloids. On the other hand, although liposome suspensions are polydisperse, they represent a very interesting model system that mimics the behavior of many biophysical systems, which show an inherent polydispersity in size, shape, and charge. For instance, liposomes and living cells can be regarded as very similar colloids, since both have a membrane (shell) formed by a phospholipid bilayer and a core inside with water in the case

of liposomes and cytoplasm in the case of cells. Moreover, the depletion attraction is an important force driving cellular organization [31] and aggregation of blood cells [32], and plays a key role in the process of macromolecular crowding [33]. Finally, liposomes are also involved in many biotechnological applications, such as drug delivery [34].

Most of the experimental works regarding charged colloid-polymer mixtures employ weakly charged colloids, so the repulsive electrostatic interaction is easily overcome by the depletion attraction induced by the polymer [4,17]. However, our experimental studies strongly differ from this procedure. Here, we study the situation where the electrostatic repulsion is strong enough to induce a highly structured initial state. After addition of the polymer coils, this repulsive interaction is counteracted by the electrostatic depletion, and the peak of the colloidal structure factor decreases accordingly. We find that the addition of short polymer coils causes a weak screening of the electrostatic repulsion. However, for long polymers the depletion attraction induces the phase separation of the mixture. With the help of the PRISM theory, we are able to estimate the depletion potential between liposomes, and compare the electrostatic effect with the entropic depletion arising with neutral polymers. The static light scattering technique (SLS) is used to follow the structural behavior of the studied mixtures.

This paper is organized as follows. In Sec. II we briefly describe the experimental setup and the characteristics of the liposome and polymer samples employed in this work. Then, Sec. III presents the theoretical method employed to calculate the effective potentials between liposomes. The results and discussion are given in Sec. IV, and the main conclusions are summarized in Sec. V.

II. MATERIALS AND METHODS

In the experiments, different concentrations of phosphatidylserine (PS) liposomes dispersed in purified water are used. Via the measure and fit of their form factor in dilute suspensions, a mean liposome radius of $R_c = 120$ nm and polydispersity (relative standard deviation) of about 0.3 are obtained. As a consequence of the extrusion procedure [35], the liposomes showed a lipid bilayer with thickness of about 4.5 nm. The liposome dispersions have a refractive index only slightly different from 1.33 (water), allowing the preparation of nearly transparent suspensions at relatively high volume fractions [36]. Consequently, these colloidal systems allow us to explore the structure and dynamics of concentrated suspensions reducing the multiple scattering effects from the analysis. Due to the specific ionization of the PS molecule in water, the liposomes are negatively charged, having an electrophoretic mobility of about -2.1×10^{-8} m^2 V^{-1} s^{-1}.

The polymers are two different polyacrylamides (Polysciences, Inc.) of molecular weights $(0.6–1) \times 10^6$ g/mol (catalog number 19901) and 5×10^6 g/mol (catalog number 21485), henceforth denoted by PAM-short and PAM-long, respectively. Their radius of gyration obtained via Zimm-plot diagrams are 25 nm (PAM-short) and 50 nm (PAM-long). Although the manufacturer presents both products as nonionic polymers, they are slightly negatively charged when immersed in distilled water at low ionic strength, due to the dissociation of the acrylamide monomers. This was experimentally confirmed by electrophoretic mobility measurements ($\mu_e \approx -0.9 \times 10^{-8}$ m^2 V^{-1} s^{-1} and $\mu_e \approx -1.1 \times 10^{-8}$ m^2 V^{-1} s^{-1} for PAM-short and PAM-long, respectively).

The light scattering experiments were performed using a three-dimensional DLS spectrometer (LS instruments, Fribourg, Switzerland) [37]. The scattered light was collected using two avalanche photodiodes and the corresponding cross-correlation function was calculated within a digital correlator. According to this design, the time-dependent contributions of multiple scattered photons can be neglected [38]. Omitting multiplicative factors, the experimental structure factor of the samples may be determined using the equation [39]

$$S(q) \propto \left(\sqrt{\frac{\langle I_A^{cp}(q) \rangle \langle I_B^{cp}(q) \rangle}{\langle I_A^{0}(q) \rangle \langle I_B^{0}(q) \rangle}} \right) \left(\frac{g_{AB}^{cp}(q,\tau=0)-1}{g_{AB}^{0}(q,\tau=0)-1} \right), \qquad (1)$$

where $\langle I_i^{cp}(q) \rangle$ is the total time-averaged intensity registered by the detectors $i = A$ and B, whereas $\langle I_i^0(q) \rangle$ corresponds to the intensity of a dilute liposome suspension. The ratio $[g_{AB}^{cp}(q,\tau=0)-1]/[g_{AB}^{0}(q,\tau=0)-1]$ corrects the magnitude of the structure factor due to the q-dependent disturbance of the multiple scattering in a cross-correlation experiment, where $g_{AB}^{i}(q,\tau) = \langle I_A^i(q,t+\tau) I_B^i(q,t) \rangle / \langle I_A^i(q,t) I_B^i(q,t) \rangle$ is the normalized cross-correlation function of the registered intensities [38,40]. In our colloid-polymer mixtures, the intensity scattered by the polymers was always very small compared to the one by liposomes, so that the experimental structure factor obtained is directly the liposome-liposome structure factor $S_{cc}(q)$.

The liposome-polymer mixtures were prepared with a fixed amount of ion-exchanger resin (Amberlite NR-150). This resin removes all the ionic impurities of the sample, so that the electrostatic interactions is reinforced. The samples were tumbled during a couple of hours after the preparation of the mixture to guarantee an efficient ion exchange. After one day, the mixtures were transferred to a thinner cylindrical quartz glass cell. This allows us to minimize the attenuation caused by the nonilluminated remaining sample and to remove the possible angular distortion of the resin in the light scattering pattern. Then, the light scattering experiments were carried out. The measurements were performed at a temperature of $T = 298$ K, within a wide angular range going from 20° to 150°, with a resolution of 2°. For PAM-short, the mixtures showed a homogeneous aspect that persisted during very long time. Quite different is the behavior found with PAM-long. In these samples, the mixtures were apparently homogeneous within the first 3 days after preparation. However, after the fourth day, a visible phase separation into a concentrated and a diluted colloidal phase was observed for the samples at larger polymer concentrations. Therefore, in these cases the measurements were performed in a metastable state where the system is under phase separation. This means that these measurements contain information about the process that finally leads to a phase separation, but they are collected during an initial period where the system is evolving slowly but still in a single phase.

III. THEORETICAL METHODS

For charged colloid-polymer mixtures, the Debye-Hückel potential [41,42] represents a suitable pair potential to model the colloid-colloid, colloid-monomer, and monomer-monomer interactions:

$$\beta V_{ij}^{\text{direct}}(r) = \begin{cases} +\infty & \text{if } r < \sigma_{ij}\left(=\frac{\sigma_i+\sigma_j}{2}\right), \\ \frac{L_B Z_i Z_j e^{-\kappa(r-\sigma_{ij})}}{r(1+0.5\kappa\sigma_i)(1+0.5\kappa\sigma_j)} & \text{if } r \geqslant \sigma_{ij}, \end{cases} \quad (2)$$

where i and j indexes can both represent colloid (liposome) or monomer. The range of the interaction is controlled by the inverse of the Debye length $\kappa = \sqrt{8\pi L_B N_A 10^3 I_{\text{ion}}}$, L_B being the Bjerrum length, N_A Avogadro's number, I_{ion} the ionic strength (in molar units), and $\beta = 1/k_B T$, where k_B Boltzmann's constant and T the absolute temperature of the system.

In order to determine the pair correlation functions, we have employed the polymer reference interaction-site model (PRISM) [43]. This is an integral equation theory based on the Ornstein-Zernike equation [44,45] (OZ). In the PRISM, the OZ equation is generalized to the molecular case introducing a new function that accounts for the correlation between atoms or sites, i.e., the intramolecular correlation, $w(r)$. With this theoretical framework, we can consider the correlation between monomers along the polymer chain [$w(r)$] and with the rest of monomers belonging to different chains [direct correlation, $c(r)$]. The PRISM can also be generalized to describe binary colloid-polymer systems. This has been successfully done for neutral [46] and charged [28] colloid-polymer mixtures. In the Fourier space, the PRISM equations are given by the following set of three coupled equations,

$$\begin{bmatrix} h_{cc}(q) & h_{cm}(q) \\ h_{cm}(q) & h_{mm}(q) \end{bmatrix} = \begin{bmatrix} 1 & 0 \\ 0 & w_m(q) \end{bmatrix} \begin{bmatrix} c_{cc}(q) & c_{cm}(q) \\ c_{cm}(q) & c_{mm}(q) \end{bmatrix} \left\{ \begin{bmatrix} 1 & 0 \\ 0 & w_m(q) \end{bmatrix} + \begin{bmatrix} \rho_c & \sqrt{\rho_c \rho_m} \\ \sqrt{\rho_c \rho_m} & \rho_m \end{bmatrix} \begin{bmatrix} h_{cc}(q) & h_{cm}(q) \\ h_{cm}(q) & h_{mm}(q) \end{bmatrix} \right\}. \quad (3)$$

In Eq. (3), $h_{ij}(q)$ and $c_{ij}(q)$ stand for the Fourier component of the total correlation function and the direct correlation function, respectively. The subscripts c and m correspond to colloids and monomers. The colloid and monomer densities are represented with ρ_c and ρ_m, respectively. $w_m(q)$ is the monomer-monomer correlation function, which accounts for the monomer connectivity along the polymer chain. It is explicitly given by the polymer form factor. Here, we have chosen Koyama's form factor [47], a semiempirical model for semiflexible polyelectrolytes which represents an interpolation between the Gaussian and the rigid chain. The model includes a parameter that takes the local rigidity of the polymer chain into account, the so-called persistence length l_p. An explicit expression of this semiempirical model can be consulted in Ref. [48].

Three additional closure equations are required to close the PRISM equation. In this study, we have proposed the HNC for liposome-liposome correlations and PY for the rest following the same arguments given in previous works [23,28,29]. The integral equations has been solved iteratively using Picard's method [49].

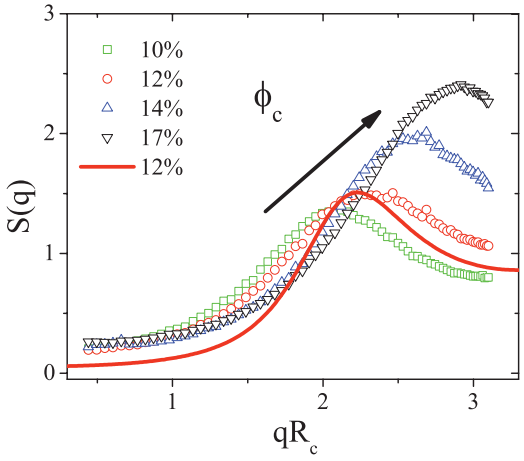

FIG. 1. (Color online) Structure factor of the liposome suspension, $S_{cc}(q)$, as a function of the dimensionless scattering vector, qR_c. The plot shows the results for different liposome concentrations ϕ_c at zero polymer concentration. The Ornstein-Zernike prediction using the HNC approximation is also shown for $\phi_c = 0.12$ as a continuous line.

IV. RESULTS AND DISCUSSION

Figure 1 depicts the experimental static structure factor $S_{cc}(q)$ calculated by means of Eq. (1) for different liposome volume fractions ($\phi_c = 0.1$, 0.12, 0.14, and 0.17) without added polymer. The experiments were performed in the presence of ion-exchanger resins, so the system can be considered at salt-free conditions. As may be observed, a well-defined peak is obtained as a consequence of the interparticle electrostatic repulsion. By increasing the liposome concentration, the peak grows and its position q^* shifts to higher q values, which agrees with the expected trend observed for fluid-like structures formed in the presence of repulsive interactions. The height of the peak reaches a value of 2.5 for the larger particle concentration.

In order to calculate the effective charge of the liposomes (Z_{eff}), we fitted these experimental structure factors using the Ornstein-Zernike integral equation [44], assuming that liposomes interact through a Yukawa interaction potential [Eq. (2)]. The integral equation was solved within the HNC approximation, which has proven to be a very accurate closure for this kind of repulsive interaction [50]. It should be noted that this fitting procedure assumes that the suspension is monodisperse. However, the real experimental samples are indeed quite polydisperse, and different particle sizes and charges may be found in the same system, leading to very broad structure factor peaks. For this reason, we only fitted the position and height of the main peak and so the effective charge should be regarded as an average value. According to this, we obtain $Z_{\text{eff}} = 230e$ for an electrolyte concentration of 10^{-6} M. In Fig. 1, the theoretical structure factor for $\phi_c = 0.12$ is shown as a dashed line. Although the position of the main peak is well reproduced by the OZ-HNC approximation (similar agreement may be found for other packing fractions), the

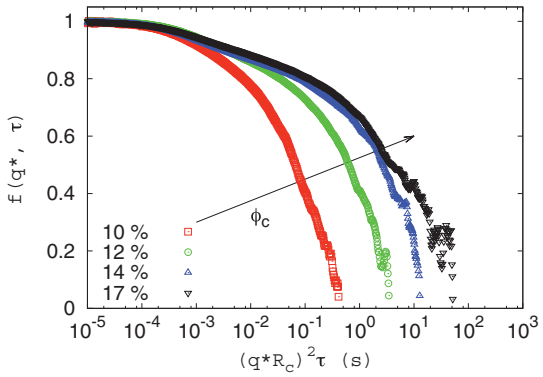

FIG. 2. (Color online) The corresponding normalized dynamic structure factor, $f(q^*,\tau)$, calculated at the main peak of the structure factor, q^*, as a function of the correlation time. The data correspond to the same samples shown in Fig. 1. The time has been rescaled for each studied liposome packing fraction.

predicted peak width is smaller than the experimental one due to polydispersity of the liposome suspensions.

For these samples, we have measured the normalized intensity cross-correlation. The dynamic structure factor $f(q^*,\tau)$ was obtained appealing to the Siegert relationship $f(q,\tau) = \sqrt{g_{AB}(q,\tau) - 1}/\sqrt{g_{AB}(q,0) - 1}$. Figure 2 shows $f(q^*,\tau)$ obtained at the main peak of the structure factor for the same liposome samples. The measurements were performed during 3500 s, which is a long enough time to obtain the proper ensemble average of the latter function. In all cases, $f(q^*,\tau)$ deviates notably from the single exponential decay of free liposomes, which is a straightforward consequence of the long-range electrostatic repulsive interactions. Indeed, $f(q^*,\tau)$ always decays to zero, with a relaxation time that increases with the liposome concentration. Although the liposome dispersions behave as a nonarrested colloidal fluid, the shape of the curves resembles the ones obtained for arrested systems. However, it should be emphasized that the interparticle repulsion is not strong enough to induce the caging of the liposomes even at the largest studied particle concentration.

Next, we study the effect of adding polymer on the liposome-liposome structure factor. Figure 3 depicts the experimental $S_{cc}(q)$ for liposome-polymer mixtures using three different liposome volume fractions for PAM-short. The curves without the added polymer are also included for comparison. As may be observed, the position of the main peak of the structure factor moves to larger q values while its height and width decreases and broadens, respectively. This effect is caused by a driving interaction counteracting the colloid-colloid electrostatic repulsion. However, it should be emphasized that such displacement is very large compared to the one obtained assuming only the screening of the double layers. This means that attractive depletion interactions are playing a key role in the peak displacement, as is demonstrated in our previous works [28,29].

For the lowest liposome concentration [Fig. 3(a)] the shift of the main peak is very important even at the smaller polymer concentrations employed in the experiments. At higher liposome packing fractions, the shift of $S_{cc}(q^*)$ becomes smaller [compare with Figs. 3(b) and 3(c)]. However, this

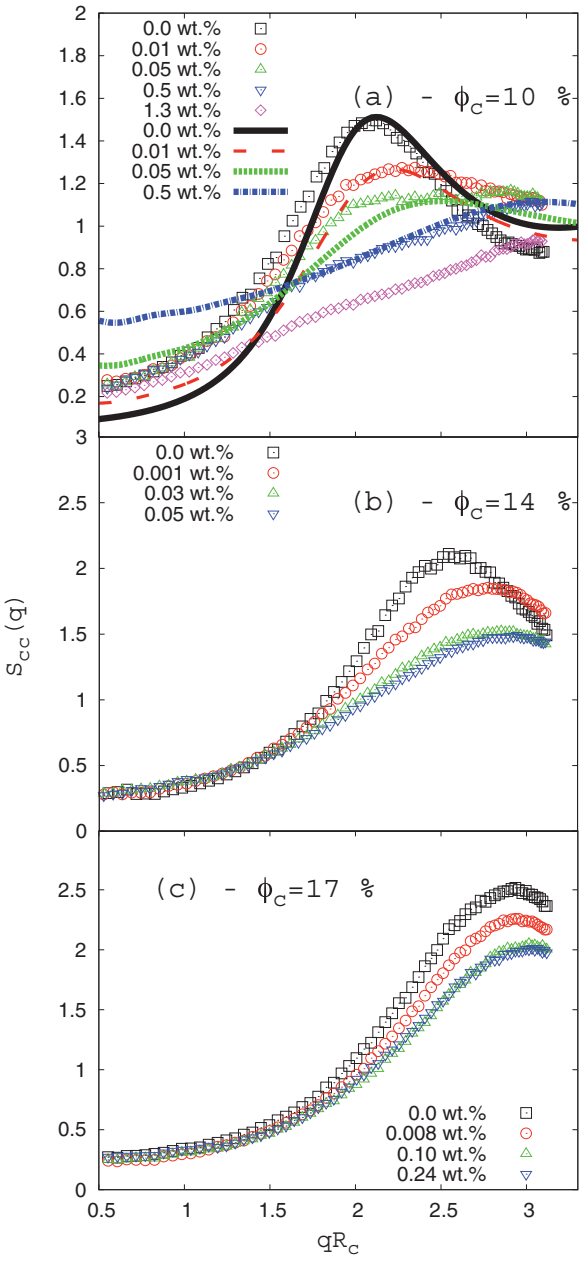

FIG. 3. (Color online) Liposome-liposome structure factor for liposome-polymer mixtures with PAM-short, at different liposome packing fractions: $\phi_c = 0.1$ (a), 0.14 (b), and 0.17 (c). The studied polymer concentrations are shown using different types of symbols (see the legends). Lines in panel (a) stand for the simulation results obtained with the interaction potential predicted by the PRISM (see legend).

does not mean that the polymer-induced effective depletion attraction is less important here, since this effective interaction only depends on the solvent and polymer properties. Indeed, for the higher liposome packing fraction, the particles are closer to each other (at zero polymer concentration) and so they feel a stronger and sharper repulsive electrostatic barrier. Under this situation, the effect of adding an attractive contribution (by increasing the polymer concentration) is only to slightly reduce this higher repulsive barrier, leading to a smaller approach between liposomes from the reference case.

The peak displacement is the consequence of the effective interactions arising in the liposome-polymer mixture. In fact, including charged polymers implies three different effects on the liposome-liposome interaction. First, the extra charge of the polymer (and the corresponding electrolyte concentration necessary for the electroneutrality of the mixture) induces a screening of the repulsive electrostatic double layers. Second, the electrostatic repulsion between liposomes and polymers causes a depletion region around the liposomes. For small polymer concentration, the size of this region is very large compared to the polymer length, leading an enhanced and long-ranged depletion attraction between particles. The origin of this depletion is mainly electrostatic. For large polymer concentrations, the screening of the double layers also reduces the range and magnitude of this electrostatic depletion. The third effect of adding the polymer is caused by the excluded volume interactions between polymers and liposomes, which induces an entropic depletion attraction between particles. The range of this depletion is roughly equal to $2R_g$ and its strength is nearly proportional to the polymer density. In this research, the large liposome packing fraction employed in the experiments suggests that both entropic and electrostatic depletion could in principle contribute to the final microstructure of the binary mixture.

The situation is very different if we use the long polymers as depletant agent. Figure 4 shows the structure factors at different liposome and polymer concentrations of PAM-long. Here, we should keep in mind that the plotted structure factors for polymer concentrations above 0.3 wt. % are nonequilibrium properties, since the system slowly evolves to a phase separation, as was mentioned in Sec. II. This means that the measurements do not have a thermodynamic interpretation. Nevertheless, these nonequilibrium structure factors still provide valuable information about the instantaneous structural behavior of the mixture before phase separation. All measurements were performed one day after the sample preparation, so they roughly correspond to the same nonequilibrium state. Then, a clear phase separation was observed 3–4 days after the measurements.

As shown by Fig. 4, the increase of the polymer concentration leads again to a weakening and displacement of the main peak of the structure factor to larger q values. Unfortunately, in most of the cases the position of the peak lies out of the experimentally accessible q range, so we are not able to exactly locate them. Despite this inconvenience, it is clear that adding long polymers induces a larger displacement of the peak than with short ones at the same polymer mass fraction.

The shift of the peak is not the only effect that appears when the long polymer is used. Moreover, we observe that increasing the concentration of PAM-long leads to a noticeable upturn of $S_{cc}(q)$ at low q values. On the one hand, this increase is in some cases an indicator of the presence of density heterogeneities in the bulk, usually found in systems where attractive interactions induce the aggregation of particles [51,52]. On the other hand, the increase of $S(q \to 0)$ may be also attributed to size or charge polydispersity effects [53,54]. As mentioned in the previous section, our liposomes are indeed polydisperse particles. Experimentally, this fact can be observed in Figs. 1 and 3. For a monodisperse stable suspension, we expect that $S(q \to 0) = 0$ (see solid line in Fig. 1 for an example of

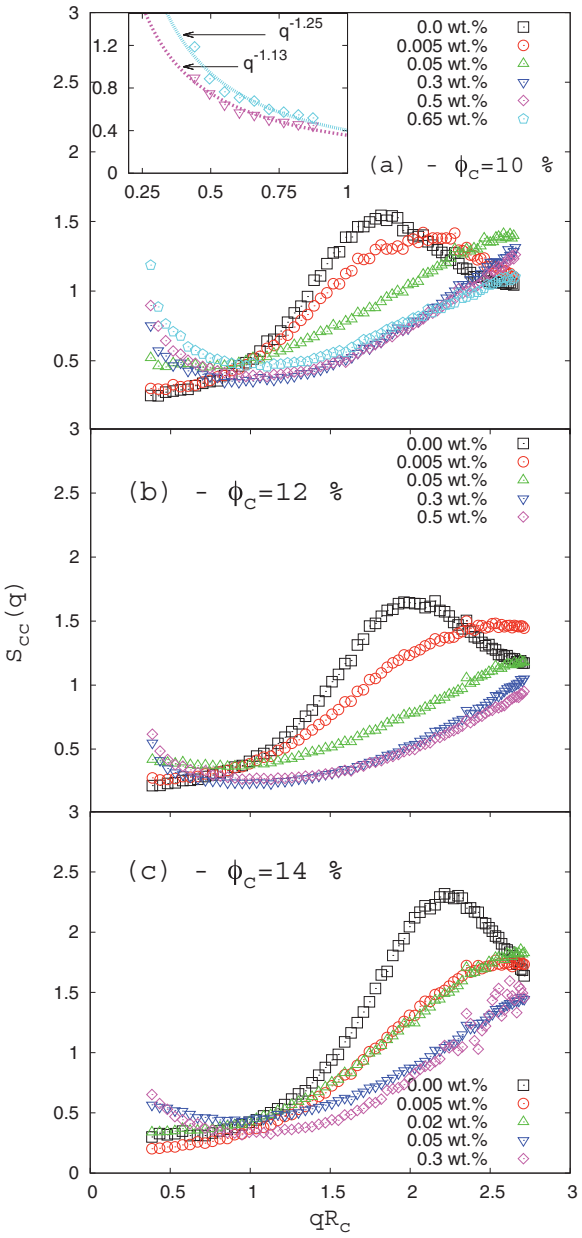

FIG. 4. (Color online) Liposome-liposome structure factor for liposome-polymer mixtures with PAM-long, at different liposome packing fractions: $\phi_c = 0.1$ (a), 0.12 (b), and 0.14 (c). Polymer concentrations are shown using different types of symbols (see the legends). The inset in panel (a) shows the $S_{cc}(q)$ at short q values for the three higher polymer concentrations: 0.3, 0.5, and 0.65 wt. %. Lines stand for the best fit using the power law $S_{cc}(q) \propto q^{-d_f}$.

monodisperse suspension). In our case, the lowest experimentally accessible data for the structure factor indicate that $S_{cc}(q \to 0) \approx 0.2$–$0.3$, which arises as a direct consequence of the polydispersity of the sample. However, the upturn at low q shown by the structure factors with PAM-long (Fig. 4) is much larger than the values for the largest polymer concentrations with PAM-short (Fig. 3). Therefore, this upturn cannot be explained in terms of polydispersity effects and it necessarily comes from the presence of aggregated clusters originated by the polymer-induced attraction between liposomes. By increasing the polymer concentration, we find a significant

growth of the upturn at low q, which is consistent with the fact that the attractive depletion interaction induces a larger concentration of clusters in the system.

In order to give a theoretical justification of peak displacement and the differences between the structure observed with PAM-short and PAM-long, we have solved the PRISM equations. This model provides detailed information about the liposome-liposome effective interaction potential, and so it may be employed to confirm whether the depletion interaction is dominated by electrostatic or entropic effects. Here, we solved the equations to calculate the liposome-liposome radial distribution function in the so-called colloidal limit. This corresponds to the limit $\rho_c \to 0$, where many-body interactions are negligible and the liposome-liposome total interaction potential $[V_{cc}^{\mathrm{Tot}}(r)]$ can be easily obtained from

$$\beta V_{cc}^{\mathrm{Tot}}(r) = -\lim_{\rho_c \to 0} \ln g_{cc}(r). \tag{4}$$

$V_{cc}^{\mathrm{Tot}}(r)$ may be decomposed in two parts: the direct term [given by the Yukawa repulsion between liposomes, Eq. (2)], and the effective contribution (arising from the polymer-induced depletion)

$$V_{cc}^{\mathrm{Tot}}(r) = V_{cc}^{\mathrm{direct}}(r) + V_{cc}^{\mathrm{eff}}(r). \tag{5}$$

Again, we neglect polydispersity effects and assume that the liposome samples are more or less represented by an equivalent monodisperse system with average particle diameter $\sigma_c = 240$ nm and average effective charge $Z_{\mathrm{eff}} = 230e$ (see Fig. 1). To model the monomer charge, we have employed the one predicted from Manning's expression $Z_m = L_B/\sigma_m$. This expression provides an estimate of the effective monomer charge caused by accumulation of counterions, condensed along the polymer chain. This approximation is valid for linear polyelectrolytes, although it has proven to perform quite well also for flexible polymers [49]. Applying Manning's model to our acrylamide monomer under low ionic conditions, the effective monomer charge is $Z_m = 0.8e$. With the use of ionic exchanger resins, the system is driven to a salt-free condition, so that $I_{\mathrm{ion}} = \frac{1}{2}(Z_c\rho_c + Z_m\rho_m + 10^{-6})$. Due to the low ionic conditions presented in our experiments, we have chosen a polymer persistence length l_p given by the sum of two different contributions: the intrinsic rigidity of the polymer, l_0, and an electrostatic contribution, $l_e = L_B/4\kappa^2\sigma_m^2$, coming from the repulsion between neighboring monomers [55]. On the one hand, the intrinsic rigidity was calculated from the radius of gyration that the polymers present in water without ionic-exchanger resins ($l_0 = 15\sigma_m$ in both cases). On the other hand, the electrostatic long-range repulsion increases the rigidity of the chain. We found $l_e = 26\sigma_m$ for 0.05 wt. % and $l_e = 9\sigma_m$ for 0.5 wt. %. We refer to Refs. [28,29] for further information about this method and the choice of the parameters.

The effective potential induced by the charged polymers is plotted in Fig. 5 for short and long polymers. The graph also includes the depletion potential obtained using an accurate semiempirical model for neutral self-avoiding polymers [56]. It should be mentioned that, although the PRISM is quite accurate for large interparticle distances, at short distances the model does not take into account the deformation of the polymer coils near the colloidal surface. Therefore, it

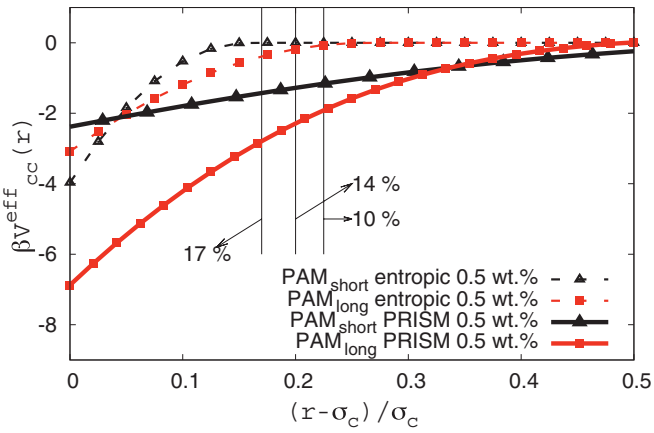

FIG. 5. (Color online) Effective interaction between liposomes induced by charged and neutral polymer in the colloidal limit for PAM-short and PAM-long (see legend) at the same polymer concentration. σ_c is the average liposome diameter.

underestimates the colloid-polymer repulsion and leads to less attractive depletion potential when colloids are very close to each other. In spite of the expected deviations at short distances, the effective potentials calculated within this approximation provide a fair description of the depletion effects arising in charged colloid-polymer mixtures. As observed, the depletion interaction induced by the charged polymers at low electrolyte concentration shows a remarkable long-range character compared to the case of neutral polymers. This long-range character is the main cause of the large shift of the structure factor peak, which cannot be explained exclusively with excluded volume interactions.

It is interesting to see that, although for neutral polymers the range of the attraction increases with the polymer size, it remains rather insensitive to this parameter for the case of charged polymers. This confirms the fact that the repulsion between charged colloids and charged polymers becomes dominated by the electrostatic counterpart at low ionic strength. Moreover, for the polymer mass fraction employed in our experiments, long polymers lead to a more efficient depletion than short ones. Figure 5 shows as vertical lines the typical distance between the surfaces of two neighboring liposomes for the three studied packing fractions. It can be clearly seen that, for short polymers, the entropic attraction is negligible and only the electrostatic effect has significant contribution. For the case of long polymers, the effective depletion potential is also mainly controlled by the electrostatic depletion, although the entropic effect also has a finite contribution, especially for $\phi_c = 0.17$.

After having found theoretical evidence of the relevance of the electrostatic depletion against the entropic one, we now study the interplay between the effective depletion attraction and the direct electrostatic repulsion. In Fig. 6, we plot the total interaction potential $\beta V_{cc}^{\mathrm{Tot}}(r)$ obtained with the PRISM for both polymers and for two polymer densities. For small polymer concentrations, depletion effects only induce a weak screening of the repulsive barrier, and so the mixture remains electrostatically stabilized. For large polymer concentration and short polymers, the interaction potential is still repulsive. However, long polymers induce a strong enough depletion

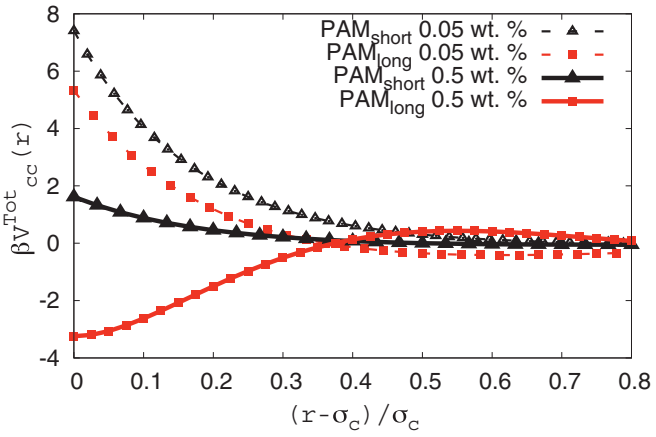

FIG. 6. (Color online) Total potential predicted by PRISM in the colloidal limit for PAM-short and PAM-long (symbol lines). Two polymer concentrations have been presented in each case (see legend). The reference direct interaction derived for a salt and polymer free liposome suspension [Eq. (3)] is also shown as a solid line.

that leads to an attractive well at contact with a repulsive barrier at intermediate distance of height $\sim 0.5 k_B T$. Under this situation, the particles are able to overcome the barrier and coagulate in the primary minimum. All these trends are in agreement with the experimental observations; i.e., samples with large concentration of long polymers finally undergo phase separation.

To check the validity of the interaction potentials predicted by the PRISM, we calculated the structure factor using Monte Carlo simulations in the canonical ensemble. In the simulations, we used $N = 600$ identical particles inside a cubic box of size $L = 14.6\sigma_c$, and applied periodic boundary conditions. The particle interactions were assumed to be given by the interaction potential obtained with the PRISM model in the colloidal limit. We have taken into account the limitation of this method showing only the real q range explored by simulation, i.e., $q_{\min} > 2\pi/L \approx 0.4\sigma_c$. In Fig. 3(a), we show the simulated $S_{cc}(q)$ (different type of lines) for $\phi_c = 0.10$. From the comparison between symbols and lines, we can say that the PRISM predictions are admissible for low colloidal concentrations. Indeed, the position of the main peak is well captured by the model, although the width of the peaks predicted by our model is in all cases smaller than the experimental one due to the inherent polydispersity of the lisosome suspension. At higher colloidal and polymer concentrations, the PRISM model loses accuracy since many-body correlation becomes very important.

The upturn of $S(q \to 0)$ observed in Fig. 4 points out the existence of an aggregation process between liposomes resulting from the competition between long-range electrostatic repulsions and the depletion attraction at large enough concentrations of long polymers. This behavior resembles the one obtained in the formation of clusters in neutral and charged binary mixtures reported experimentally [6–8] and by computer simulations [16,51]. In this framework, the aggregation process induced by depletion attractions and the different routes leading to the gelation process are still controversial subjects [13,16]. There is a wide literature focused on mixtures of hard-sphere colloids and nonadsorbing uncharged polymers where the entropic depletion is the only mechanism causing the phase separation [6–8,19]. However, less is known about the aggregation process arising in binary mixtures when both colloids and polymers are charged.

In the inset of Fig. 4(a), we provide experimental evidence of this aggregation process. As usually, the cluster morphology is characterized by means of its fractal dimension d_f. It has been calculated from the fitting of the $S_{cc}(q)$ using the power law

$$S(q) \sim q^{-d_f}, \quad R_{\text{cluster}}^{-1} \leqslant q \leqslant R_c^{-1}, \tag{6}$$

where R_{cluster} is the hydrodynamic cluster radius, and R_c the average particle radius. Given the angular limitation to reach small q scattering vectors (the standard procedure establishes that the fit must be performed at least along a decade) the extracted fractal dimensions can only be regarded as approximate values. Nevertheless, the results represent a qualitative estimation that helps to understand the mechanisms involved in the aggregation process. From the fitting at the low-q region of $S_{cc}(q)$, we find that the clusters have fractal dimensions, which could correspond to linear structures. In this sense, our experimental data agree with the observations of Campbell [13], who obtains chainlike aggregates, and Sedgwick [5], where mixtures of particles and chainlike clusters are found. In fact, these results are also consistent with the theoretical predictions obtained with the PRISM. The reminiscent electrostatic repulsive barrier between liposomes observed in Fig. 6 followed by an attractive well at short distances favors the aggregation at the tips of the cluster, since this configuration minimizes the net repulsion between particles. Moreover, due to the short-range London–van der Waals attractions, the bonds between liposomes forming the cluster become almost irreversible, impeding the particle reorganization inside the aggregate.

Our study on charged colloid-polymer mixtures at large packing fraction of colloids and polymers draws a complex scenario. This is illustrated in Fig. 7. Adding PAM-short and small amounts of PAM-long, liposomes become closer each other by a driving interaction counteracting the electrostatic repulsion. Therefore, there is only one relevant distance that

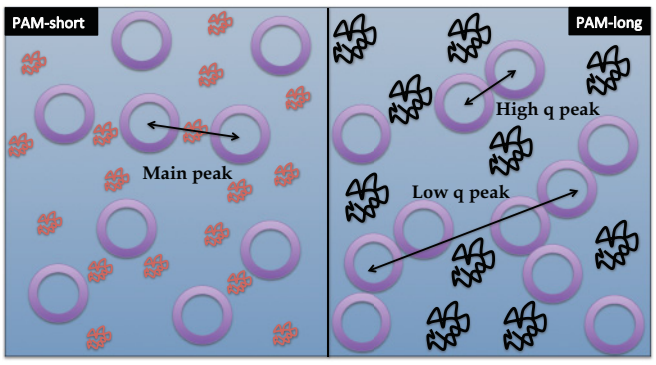

FIG. 7. (Color online) This picture illustrates the microscopic rearrangement of the liposome under the presence of PAM-short (liquid-like phase) and PAM-long (aggregated liposomes in a fluid phase). In each panel, the relevant length scales between liposomes are represented with a solid line.

corresponds to the main peak of the structure factors shown in Fig. 3 (liposome-liposome). Adding large amounts of PAM-long, the induced attraction is strong enough to overcome the repulsive barrier at intermediate distances leading to the aggregation of liposomes. The clusters define a new relevant length between them at low q, which is related to the upturn at short q values in the structure factor. The liposome-liposome distance is now represented in the peak that shifts to high q values. The distance between liposomes is now quite small and so the peak is out of the our experimental q range.

V. CONCLUSIONS

It has been shown that the addition of charged polymers to charged stabilized liposome suspensions at low electrolyte concentration leads to significant changes in the structure of liposome suspensions. The displacement of the main peak of the structure factor can be only explained in terms of a long-range electrostatically enhanced effective depletion attraction. This depletion arises from the fact that charged polymers are depleted from the surrounding region around the liposomes, as a consequence of the electrostatic liposome-polymer repulsion.

The theoretical predictions obtained with the PRISM suggest that the entropic depletion effects are small compared to the electrostatic ones. Moreover, the interaction potential provided by this model in the colloidal limit shows the interplay between electrostatic repulsion and the depletion attraction. In particular, for strong enough electrostatic depletion (large packing fraction of PAM-long), the theoretical results predict an attractive well at short interparticle distances that leads to the destabilization of the mixture. This conclusion agrees with the experimental observations found for large concentrations of long polymers. Finally, the experimental data also suggest that under this nonequilibrium situation, the aggregation between liposomes leads to the formation of linear shape cluster. We interpret this behavior in terms of a residual electrostatic repulsion that emphasized the aggregation at the tips of the clusters.

It is important to point out some limitations of the model. First, the PRISM predictions are obtained in the limit of very small density of liposomes. Although this is an elegant method to calculate effective pair potentials, it does not account for many-body interactions. At the high liposome concentration employed in this work, we expect that three or more body contributions will be also involved in the structure of the mixture. Second, the model also ignores polydispersity effects. In spite of these inconveniences, the PRISM approximation still represents a useful qualitative approximation that has proven fruitful in describing the depletion effects arising in charged mixtures. Future works will improve these points with more sophisticated methods, and will include studies of binary mixtures with different chain rigidity.

ACKNOWLEDGMENTS

The authors are grateful to "MICINN" (Projects No. MAT2009-13155-C04-02 and No. MAT2009-13155-C04-03) ERDF Funds and "Junta de Andalucía" (Excellency Projects No. P07-FQM-02517 and No. P07-FQM-02496) for financial support. We would also like to thank R. Barnadas for advice on the synthesis of PS liposomes.

[1] W. C. K. Poon, J. Phys.: Condens. Matter **14**, R859 (2002).
[2] A. P. Gast, W. B. Rüssell, and C. K. Hall, J. Colloid Interface Sci. **96**, 1977 (1983).
[3] H. N. W. Lekkerkerker, W. C. Poon, P. N. Pusey, A. Stroobants, and P. B. Warren, Europhys. Lett. **20**, 559 (1992).
[4] P. N. Segre, V. Prasad, A. B. Schofield, and D. A. Weitz, Phys. Rev. Lett. **86**, 6042 (2001).
[5] H. Sedgwick, S. U. Egelhaaf, and W. C. K. Poon, J. Phys.: Condens. Matter **16**, S4913 (2004).
[6] S. Manley, H. M. Wyss, K. Miyazaki, J. C. Conrad, V. Trappe, L. J. Kaufman, D. R. Reichman, and D. A. Weitz, Phys. Rev. Lett. **95**, 238302 (2005).
[7] P. J. Lu, J. C. Conrad, H. M. Wyss, A. B. Schofield, and D. A. Weitz, Phys. Rev. Lett. **96**, 028306 (2006).
[8] P. J. Lu, E. Zaccarelli, F. Ciulla, A. B. Schofield, F. Sciortino, and D. Weitz, Nature (London) **453**, 499 (2008).
[9] M. Laurati, G. Petekidis, N. Koumakis, F. Cardinaux, A. B. Schofield, J. M. Brader, M. Fuchs, and S. U. Egelhaaf, J. Chem. Phys. **130**, 134907 (2009).
[10] S. Asakura and F. Oosawa, J. Chem. Phys. **22**, 1255 (1954); J. Polymer Sci. **33**, 183 (1958).
[11] A. Vrij, Pure. Appl. Chem. **48**, 471 (1976).
[12] S. A. Shah, S. Ramakrishnan, Y. L. Chen, K. S. Schweizer, and C. F. Zukoski, Langmuir **19**, 5128 (2003).
[13] A. I. Campbell, V. J. Anderson, J. S. van Duijneveldt, and P. Bartlett, Phys. Rev. Lett. **94**, 208301 (2005).
[14] A. Stradner, H. Sedgwick, F. Cardinaux, W. C. K. Poon, S. Egelhaaf, and P. Shurtenberger, Nature (London) **432**, 492 (2004).
[15] C. P. Royall, D. G. A. L. Aarts, and H. Tanaka, J. Phys.: Condens. Matter **17**, S3401 (2005).
[16] F. Sciortino, S. Mossa, E. Zaccarelli, and P. Tartaglia, Phys. Rev. Lett. **93**, 055701 (2004).
[17] T. H. Zhang, J. Groenewold, and W. K. Kegel, Phys. Chem. Chem. Phys. **11**, 10827 (2009).
[18] C. L. Klix, C. P. Royall, and H. Tanaka, Phys. Rev. Lett. **104**, 165702 (2010).
[19] C. Gögelein, G. Nägele, J. Buitenhuis, R. Tuinier, and J. K. Dhont, J. Chem. Phys. **130**, 204905 (2009).
[20] K. P. Velikov, C. G. Christora, R. P. A. Dullens, and A. van Blaaderen, Science **296**, 106 (2002).
[21] A. Y.-G. Fuh, J. G. Chen, S.-Y. Huang, and K.-T. Cheng, Appl. Phys. Lett. **96**, 051103 (2010).
[22] T. H. Windhom and C. A. Cain, IEEE Trans. Biomed. Eng. **26**, 148 (1979).
[23] L. Belloni and P. G. Ferreira, Philos. Trans. R. Soc. London A **359**, 867 (2001).

[24] A. R. Denton and M. Schmidt, J. Chem. Phys. **122**, 2449111 (2005).
[25] J. Y. Walz and A. Sharma, J. Colloid Interface Sci. **168**, 485 (1994).
[26] O. Mondain-Monval, F. Leal-Calderón, J. Philip, and J. Bibette, Phys. Rev. Lett. **75**, 3364 (1995).
[27] L. Helden, G. H. Koenderink, P. Leiderer, and C. Bechinger, Langmuir **20**, 5662 (2004).
[28] M. Peláez-Fernández, A. Moncho-Jordá, and J. Callejas-Fernández, Europhys. Lett. **90**, 46005 (2010).
[29] M. Peláez-Fernández, A. Moncho-Jordá, and J. Callejas-Fernández, J. Chem. Phys. **134**, 054905 (2011).
[30] S. Buzzaccaro, R. Piazza, J. Colombo, and A. Parola, J. Chem. Phys. **132**, 124902 (2010).
[31] D. Marenduzzo, K. Finan, and P. R. Cook, J. Cell Biol. **175**, 681 (2006).
[32] B. Neu and H. J. Meiselman, Biophys. J. **83**, 2482 (2002).
[33] S. B. Zimmerman and A. P. Minton, Annu. Rev. Biophys. Biomol. Struct. **22**, 27 (1993).
[34] P. Goyal, K. Goyal, S. G. V. Kumar, A. Singh, O. P. Katare, and D. N. Mishra, Acta Pharm. **55**, 1 (2005).
[35] C. Haro-Peréz, Ph.D. thesis, University of Granada, 2005.
[36] C. Haro-Pérez, L. F. Rojas-Ochoa, V. Trappe, R. Castañeda-Priego, J. Estelrich, M. Quesada-Pérez, J. Callejas-Fernéndez, and R. Hidalgo-Álvarez, in *Structure and Functional Properties of Colloidal Systems*, edited by R. Hidalgo-Álvarez, Surfactant Science Series, Vol. 146 (CRC Press, Boca Raton, 2010), p. 77.
[37] C. Urban, J. Colloid Interface Sci. **207**, 150 (1998).
[38] G. Phillies, J. Chem. Phys. **74**, 260 (1980).
[39] A. Moussaïd and P. N. Pusey, Phys. Rev. E **60**, 5670 (1999).
[40] K. Schätzel, J. Mod. Opt. **38**, 1849 (1991).
[41] P. W. Debye and E. Hückel, Z. Phys. **24**, 185 (1923).
[42] B. J. Berne and R. Pecora, *Dynamic Light Scattering* (Wiley, New York, 1976).
[43] J. G. Curro and K. S. Schweizer, Macromol. **20**, 1928 (1987).
[44] J. P. Hansen and I. R. McDonald, *Theory of Simple Liquids* (Academic, New York, 1976).
[45] D. Chandler, in *Studies in Statistical Mechanics*, Vol. 8, edited by E. Montroll and J. L. Lebowitz (North Holland, Amsterdam, 1982), p. 274.
[46] A. Yethiraj, C. K. Hall, and R. Dickman, J. Colloid Interface Sci. **151**, 102 (1992).
[47] R. Koyama, Macromol. **19**, 178 (1986).
[48] K. G. Honnell, J. G. Curro, and K. S. Schweizer, Macromol. **23**, 3496 (1990).
[49] M. Dymitrowska and L. Belloni, J. Chem. Phys. **109**, 4659 (1998); **111**, 6633 (1999).
[50] J. M. Méndez-Alcaraz, B. D'Aguanno, and R. Klein, Langmuir **8**, 2913 (1992).
[51] E. Zaccarelli, S. Andreev, F. Sciortino, and D. R. Reichman, Phys. Rev. Lett. **100**, 195701 (2008).
[52] G. Nägele, Phys. Rep. **272**, 215 (1996).
[53] B. D'Aguanno and R. Klein, J. Chem. Soc., Faraday Trans. **87**, 379 (1991).
[54] C. Haro-Pérez, M. Quesada-Pérez, J. Callejas-Fernández, E. Casals, J. Estelrich, and R. Hidalgo-Álvarez, J. Chem. Phys. **118**, 5167 (2003).
[55] E. Buhler and F. Boué, Eur. Phys. J. E **10**, 89 (2003).
[56] A. Louis, J. Chem. Phys. **117**, 1893 (2002).